Design and Implementation of an Unmanned Water Quality Monitoring Vessel Based on Intelligent Navigation Control

Liu Yu[1] and Suchada Sitjongsataporn[2,*]

[1] The Electrical Engineering Graduate Program, Faculty of Engineering and Technology
Mahanakorn University of Technology International College (MUTIC)
Mahanakorn University of Technology, Bangkok, Thailand
[2]Department of Electronic Engineering, School of Electrical and Electronic Engineering (SEE)
Faculty of Engineering and Technology, Mahanakorn University of Technology, Bangkok, Thailand

Abstract: With the increasing severity of water pollution, traditional manual sampling and laboratory testing methods can no longer meet the requirements of real-time and large-scale monitoring. As a novel monitoring platform, unmanned water quality monitoring vessels are characterized by high mobility, strong automation, and flexibility, and have been increasingly applied in smart aquaculture, lake management, and water resource protection. This paper proposes an unmanned water quality monitoring vessel based on a dual-control architecture integrating APM2.8 and STM32. The system innovatively employs the APM2.8 autopilot for navigation control and path planning, combining GPS and inertial sensors to achieve high-precision autonomous navigation. Meanwhile, an STM32F103 microcontroller is adopted as the water quality monitoring core to realize real-time acquisition and processing of multiple parameters, including temperature, pH, TDS, turbidity, and water depth. A dual-channel communication structure consisting of LoRa and WiFi is designed to support long-range remote monitoring and short-range high-speed interaction. Experimental results show that the proposed system achieves superior performance in trajectory tracking accuracy, task execution efficiency, and data acquisition reliability. The average trajectory deviation is less than 0.3 m, and the sensor measurement error is controlled within the design range. Compared with traditional single-controller architectures, the proposed system demonstrates significant improvements in autonomy, stability, and scalability.

***Index Terms*—APM2.8, autonomous navigation, dual-control architecture, STM32, unmanned water quality monitoring vessel.**

I. Introduction

In recent years, water pollution has become increasingly severe, posing critical challenges to environmental protection and water resource management [1]. Achieving efficient, real-time, and dynamic water quality monitoring has become a key research topic. [2] Traditional manual sampling methods are limited by time and labor, and cannot satisfy the requirements for continuous monitoring of large-scale water bodies [3]. The emergence of unmanned water quality monitoring vessels provides a new solution to this problem [4-5]. However, many existing unmanned vessels still rely primarily on remote control or fixed-point monitoring, lacking efficient autonomous navigation and multi-point sampling capabilities.

To address the insufficient intelligence of current systems, this paper proposes an unmanned water quality monitoring vessel based on a dual-control architecture of APM2.8 and STM32. The APM2.8 autopilot is responsible for navigation and path control, while the STM32 microcontroller manages water quality monitoring and data acquisition. By decoupling navigation control and environmental monitoring, the dual-control architecture enhances system stability and scalability, enabling high-precision autonomous navigation and multi-parameter monitoring in complex water environments.

Received: 26 September 2025
Revised: 10 December 2025
Accepted: 11 December 2025

*Corresponding author: Assoc.Prof. Dr. Suchada Sitjongsataporn, Department of Electronic Engineering, School of Electrical and Electronic Engineering (SEE), Bangkok, Thailand. (Email: ssuchada@mut.ac.th).

II. System Overview

The system consists of the hull structure, navigation control unit, water quality monitoring unit, communication module, and power management unit. Each part plays an essential role in ensuring the stable operation of the vessel during autonomous monitoring tasks.

APM2.8 Autopilot: Serves as the navigation control core, responsible for path planning, attitude solution, and propulsion control. By integrating GPS and IMU data, it ensures accurate trajectory tracking and reliable maneuvering under dynamic water conditions.

STM32F103 Microcontroller: Acts as the monitoring

core, responsible for multi-parameter data acquisition and upload. It interfaces with temperature, pH, TDS, turbidity, and depth sensors, applying filtering and anomaly detection algorithms to improve data reliability.

Communication Module: Utilizes dual channels of LoRa and WiFi, enabling long-range low-power transmission for field monitoring and short-range high-speed interaction for local debugging and visualization.

Power System: Employs a hybrid power supply of lithium batteries and solar panels, with voltage regulation circuits to ensure stable operation and extended endurance.

Together, these subsystems form a dual-control architecture that balances intelligent navigation with precise water quality monitoring. The overall system block diagram is shown in Figure 1.

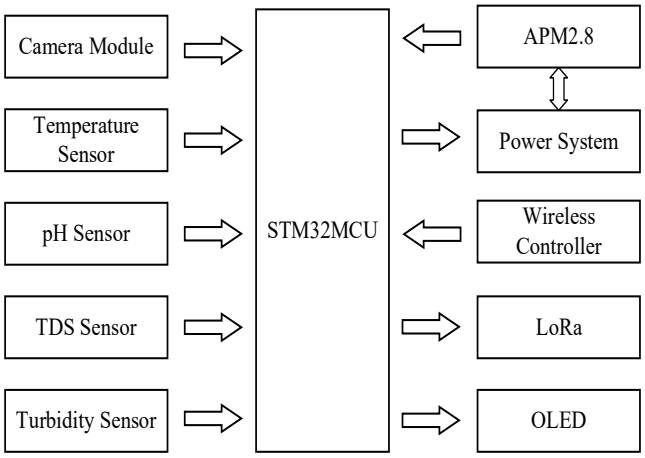

Fig. 1. System Block Diagram

III. Hardware Design

A. APM2.8 Navigation Control Unit

The APM2.8 integrates an MPU6000 six-axis IMU, barometer, GPS interface, and multi-channel PWM outputs [6]. Running on ArduPilot firmware, it performs trajectory planning and attitude control. PWM signals are used to drive DC motors and servos, enabling differential steering and autonomous navigation. The module is shown in Figure 2.

Fig. 2. APM 2.8 Flight Controller [6]

B. STM32 Water Quality Monitoring Unit

The STM32 microcontroller acquires and processes data from multiple sensors, including temperature, pH, TDS, turbidity, and water depth. It implements data filtering and anomaly detection before transmitting data via LoRa or WiFi. The module is shown in Figure 3.

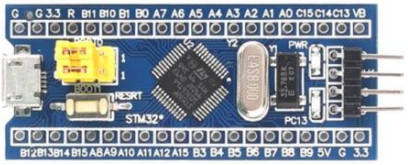

Fig. 3. STM32F103C8T6 MCU

C. Motor and Drive Module

The propulsion system consists of dual DC gear motors (JGB37-520), controlled by a TB6612FNG dual-channel motor driver [7]. This configuration provides reliable forward, reverse, and turning operations, enabling smooth navigation in various water conditions. The module is shown in Figure 4.

Fig. 4. TB6612FNG module

D. Communication Module

To ensure stable long-range communication, the system adopts a LoRa-based communication module (DX-LR01). LoRa technology provides low-power, long-distance wireless transmission, making it suitable for open water environments where cellular or WiFi coverage may be limited. Data collected by STM32 are transmitted to the remote monitoring terminal through LoRa, ensuring robust communication over several kilometers [8-9]. The module is shown in Figure 5.

Fig. 5.DX-LR01 Lora module

E. Power Management

The vessel employs a hybrid power supply consisting of lithium batteries and solar panels. The LM2596S-ADJ DC-DC converter provides stable 5 V and 3.3 V regulated outputs for different subsystems [10]. This design ensures continuous operation for extended monitoring missions and prevents undervoltage or overload damage to electronic components shown in Figure 6.

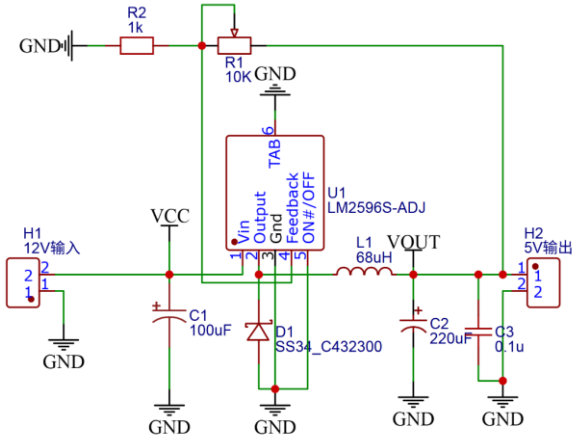

Fig. 6. Schematic diagram of power supply circuit

IV. Software Design

A. APM2.8 Navigation Control Logic

Based on the ArduPilot firmware, multiple waypoints are configured using Mission Planner. The APM2.8 executes trajectory tracking and obstacle avoidance during navigation. The operation interface is shown in Figure 7.

In the Mission Planner interface for APM2.8 as follows:

(1) the connect button is used to establish or disconnect communication with the ground station;

(2) the link status display shows signal strength and data transmission quality;

(3) the function menu bar allows flight mode selection and common operations;

(4) the hardware and sensor configuration section provides access to firmware installation and calibration settings;

(5) the radio calibration interface displays real-time channel inputs and completes range calibration to ensure accurate command recognition by the flight controller.

Fig. 7. Operation interface

B. STM32 Monitoring Logic

The STM32 runs a state machine to initialize sensors, collect and filter data, perform anomaly detection, and package the results for transmission via LoRa/WiFi. The programming interface is shown in Figure 9.

C. Dual-Control Cooperation Logic

When the STM32 detects abnormal water quality parameters, it sends instructions to the APM2.8 via UART. This can trigger additional sampling or path adjustment in the abnormal area, achieving dynamic cooperation between navigation and monitoring tasks.

The workflow of the data transmission process is illustrated in Figure 8. The system begins with initialization, followed by continuous reception of sensor data. The collected water quality data are displayed through the serial port, enabling real-time monitoring and logging. The system then checks whether control instructions are required. If no instruction is detected, the system loops back to data reception and continues normal monitoring. If an instruction is triggered, the STM32 transmits control commands to the APM2.8, which then adjusts the vessel's navigation behavior accordingly. This closed-loop design ensures that monitoring and navigation tasks are dynamically coordinated, enhancing the adaptability and intelligence of the unmanned vessel.

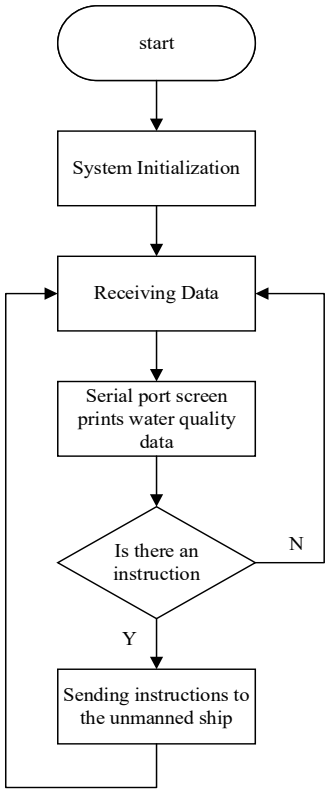

Fig. 8. Data transmission flow chart

V. System Testing and Experimental Results

A. Navigation Accuracy Test

As shown in Figure 10, five marker points were deployed in the artificial lake to evaluate the trajectory tracking performance of the vessel. The planned trajectory and the

actual trajectory obtained through GPS measurements were compared, as shown in Table I.

```
36    while (1)
37    {
38        /*TMP*/
39      temper=DS18B20_GetTemperture();
40      OLED_ShowNum(1,8,temper,2);
41        OLED_ShowString(1,10,".");
42      OLED_ShowNum(1,11,(uint16_t)(temper*10)%10,1);
43        OLED_ShowNum(1,12,(uint16_t)(temper*100)%10,1);
44      /*pH*/
45        AD1 = AD_GetValue(ADC_Channel_1);
46      //Start ADC once, convert channel 1
47      pH_Voltage = (float)AD1 / 4095 * 3.3;
48      //The AD value is linearly converted to the range of 0~3.3, indicating voltage
49      pHValue = -5.7541 * pH_Voltage + 16.654;
50        OLED_ShowNum(2, 10, pHValue, 1);
51      //Displays the integer part of the pH value
52        OLED_ShowString(2,11,".");
53      OLED_ShowNum(2, 12, (uint16_t)(pHValue * 100) % 100, 2);
54      //Display the decimal part of the pH value
55      /*TDS*/
56        AD2 = AD_GetValue(ADC_Channel_2);    //Start ADC once, convert channel 2
57        TDS_Voltage = (float)AD2 / 4096 * 3.3; //AD conversion
58        TDSValue = 66.71 * TDS_Voltage * TDS_Voltage * TDS_Voltage
59                 - 129.73 * TDS_Voltage * TDS_Voltage
60                 + 428.7 * TDS_Voltage;
61        OLED_ShowNum(3, 10, TDSValue, 4);       //Displays the integer part of the pH value
62        /*TU*/
63        AD3 = AD_GetValue(ADC_Channel_3);    //Start ADC once, convert channel 2
64        TU_Voltage = (float)AD3 / 4096 * 3.3; //AD conversion
65        TUValue = - 865.68 * TU_Voltage * 2 + 1655.4;//1655.40
66        if(TUValue<=0){TUValue=0;}
67      if(TUValue>=3000){TUValue=3000;}
68        OLED_ShowNum(4, 10, TUValue, 4);        //Displays the integer part of the TU value
69        /*Serial port 3 data receiving*/
70        if (Seria3_GetRxFlag() == 1)  //If a data packet is received
71    {
83        /*Serial port 1 data reception*/
84        if (Serial_GetRxFlag() == 1)  //If a data packet is received
85    {
```

Fig. 9. Programming interface

Fig. 10. Fixed-point navigation

TABLE I
TRAJECTORY COMPARISON TEST TABLE

Sampling Point	Planned Coordinates	Actual Coordinates	Error (%)
P1	(30.000, 120.000)	(30.001, 119.999)	0.60%
P2	(30.005, 120.002)	(30.006, 120.003)	0.73%
P3	(30.010, 120.005)	(30.011, 120.004)	0.63%
P4	(30.015, 120.008)	(30.016, 120.010)	0.80%
P5	(30.020, 120.012)	(30.019, 120.011)	0.65%

The results indicate that the maximum positioning error among the five marker points was 0.80%, while the average error remained below 0.70%, demonstrating that the navigation system based on the APM2.8 autopilot achieved stable and precise trajectory tracking.

The percentage-based error representation highlights that the vessel maintained its trajectory with high accuracy across all marker points, keeping deviations consistently under 1%. This level of precision ensures that navigation tasks are executed as planned, providing a reliable basis for subsequent monitoring operations.

B. Multi-Point Navigation Task

To further evaluate the autonomous navigation capability of the vessel, a multi-point navigation experiment was conducted in an artificial lake. Five marker points were predefined along a closed loop trajectory, and the vessel was tasked to navigate through these points sequentially under fully autonomous control. The mission plan was uploaded via Mission Planner, and the APM2.8 autopilot executed waypoint tracking using integrated GPS and IMU data. The hull navigation diagram is shown in Figure 11.

During the experiment, buoys were deployed along the trajectory to simulate obstacles. When encountering these buoys, the APM2.8 successfully replanned local paths and executed smooth avoidance maneuvers without significant deviation from the overall trajectory. The actual arrival times at each marker point were close to the expected values, with timing errors maintained within 5% as summarized in Table II.

TABLE II
SAILING TIME COMPARISON TABLE

Point	Expected arrival (s)	Actual arrival (s)	Error (%)
P0–P1	120	125	4.17%
P1–P2	240	247	2.92%
P2–P3	360	365	1.39%
P3–P4	480	489	1.88%
P4–P5	600	609	1.50%

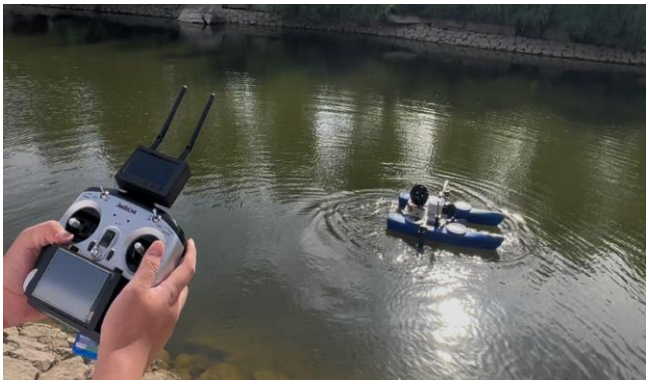

Fig. 11. Obstacle Avoidance

C. Water Quality Monitoring Accuracy Test

To evaluate the accuracy of the onboard monitoring system, laboratory instruments were employed as reference standards, as illustrated in Figure 12.

Water samples were measured simultaneously by the laboratory instruments and the sensors integrated into the vessel. The comparison between the two sets of measurements is summarized in Table III.

Fig. 12. Sensor testing

TABLE III
SENSOR TEST DATA COMPARISON

Parameter	Laboratory Value	Vessel Measurement	Error (%)
Temperature (℃)	25.0	24.8	0.8 %
pH	7.00	6.96	0.57 %
TDS (ppm)	350	343	2.00 %
Turbidity (NTU)	200	207	3.50 %
Depth (m)	5.0	4.9	2.00 %

The results indicate that the measurement errors of all sensors remained within ±3.5%, which is acceptable for practical water environment monitoring. The turbidity sensor exhibited the largest deviation (3.5%), while temperature and pH sensors showed the highest accuracy with errors below 1%. These findings confirm that the STM32-based monitoring unit provides reliable real-time water quality data acquisition.

Compared with traditional single-controller systems, the proposed dual-control architecture demonstrates significant advantages. By separating navigation (APM2.8) from monitoring tasks (STM32), the vessel maintains high navigation precision while ensuring accurate sensor performance. This design effectively balances operational stability and measurement reliability, providing a solid foundation for long-term autonomous monitoring applications.

VI. Conclusion

This paper presents the design and implementation of an unmanned water quality monitoring vessel based on a dual-control architecture combining APM2.8 and STM32. The layered control design enables APM2.8 to perform intelligent navigation while STM32 executes water quality monitoring and data transmission. Experiments demonstrate that the system achieves high trajectory accuracy, reliable sensor performance, reasonable power consumption, and long endurance. The proposed approach meets the requirements of smart aquaculture and water environment management, providing a promising solution for real-time dynamic water quality monitoring.

References

[1] Q. -D. Chen et al., "Vector Field-Based Guidance Method for Collision Avoidance of Unmanned Surface Vehicles," 2023 IEEE Underwater Technology (UT), Tokyo, Japan, pp. 1-7, 2023.

[2] S. Madhusudhana, D. A. Soto and T. Gedamke, "Automating Lobster Length Assessments Towards Facilitating Rapid Fisheries-Assisted Sampling," *OCEANS 2024 - Halifax*, Halifax, NS, Canada, pp. 1-5,2024.

[3] K. Kim, "Experimental Deployment of Automatic Buoy Identification Monitoring System (ABIMS) for Sustainable Fishery and Healthy Oceans," *OCEANS 2024 - Singapore*, Singapore, Singapore, pp. 1-5, 2024.

[4] U. G. Sharanya, K. M. Birabbi, B. H. Sahana, D. M. Kumar, N. Sharmila and S. Mallikarjunaswamy, "Design and Implementation of IoT-based Water Quality and Leakage Monitoring System for Urban Water Systems Using Machine Learning Algorithms," *2024 Second International Conference on Networks, Multimedia and Information Technology (NMITCON)*, Bengaluru, India, pp. 1-5, 2024.

[5] P. K. Malik, P. Malik, G. R. Kumar, Sneha, R. Abraham and R. Singh, "Design and Implementation of a LoRa-Based Water Quality Monitoring System," *2023 3rd International Conference on Advancement in Electronics & Communication Engineering (AECE)*, GHAZIABAD, India, pp. 120-124, 2023.

[6] G. V. S. Lohit and D. Bisht, "Seed Dispenser using Drones and Deep Learning Techniques for Reforestation," *2021 5th International Conference on Computing Methodologies and Communication (ICCMC)*, Erode, India, 2021, pp. 1275-1283.

[7] S. Xinzheng, X. Luyan, W. Wancheng, L. Xiaoyu, N. Tianqi and W. Yichen, "Design of Intelligent Drug Delivery Vehicle Based on MSP430 MCU," *2022 5th International Conference on Energy, Electrical and Power Engineering (CEEPE)*, Chongqing, China, 2022, pp. 1068-1073.

[8] Y. Liu, J. Cai and M. Qiu, "Research on low-power and low-cost smart animal husbandry positioning system based on LoRa transmission," *2025 5th International Symposium on Computer Technology and Information Science (ISCTIS)*, Xi'an, China, 2025, pp. 571-575.

[9] W. Chanwattanapong, S. Hongdumnuen, B. Kumkhet, S. Junon and P. Sangmahamad, "LoRa Network Based Multi-Wireless Sensor Nodes and LoRa Gateway for Agriculture Application," *2021 Research, Invention, and Innovation Congress: Innovation Electricals and Electronics (RI2C)*, Bangkok, Thailand, 2021, pp. 133-136.

[10] K. -T. Hsu, Z. -Y. Wang and W. -P. Chen, "Design of Intelligent Energy-Saving Controller Using Faucet," *2022 IEEE 4th Eurasia Conference on Biomedical Engineering, Healthcare and Sustainability (ECBIOS)*, Tainan, Taiwan, 2022, pp. 122-125.

Liu Yu received his B.Eng. degree in Qingdao Huanghai University, China in 2022. Currently, he holds a master's degree. in electrical engineering (electronic) in Mahanakorn University of Technology, Thailand. His research interests are embedded system, and automatic control system.

Suchada Sitjongsataporn received her B.Eng. (first-class honors) and D.Eng. degrees in Electronic Engineering from the Mahanakorn University of Technology, Bangkok, Thailand in 2002 and 2009, respectively. She has worked as a lecturer at the department of electronic engineering, Mahanakorn University of Technology since 2002. Currently, she is an Associate Professor in electronic engineering, the Assistant President for Research and Dean of Graduate College in the Mahanakorn University of Technology. Her research interests are in mathematical and statistical models in the area of adaptive signal processing for communications, networking, embedded system, and image and video processing.